

Field scale spatial wheat yield forecasting system under limited field data availability by integrating crop simulation model with weather forecast and satellite remote sensing

Rajkumar Dhakar ^a, Vinay Kumar Sehgal ^{a,*}, Debasish Chakraborty ^{a,b}, Rabi Narayan Sahoo ^a, Joydeep Mukherjee ^a, Amor V.M. Ines ^c, Soora Naresh Kumar ^d, Paresh B. Shirasath ^e, Somnath Baidya Roy ^f

^a Division of Agricultural Physics, ICAR - Indian Agricultural Research Institute, New Delhi, India

^b ICAR Research Complex for NEH Region, Umiam, Meghalaya, India

^c International Research Institute for Climate and Society, Columbia University, NY, USA

^d CESCRA, ICAR - Indian Agricultural Research Institute, New Delhi, India

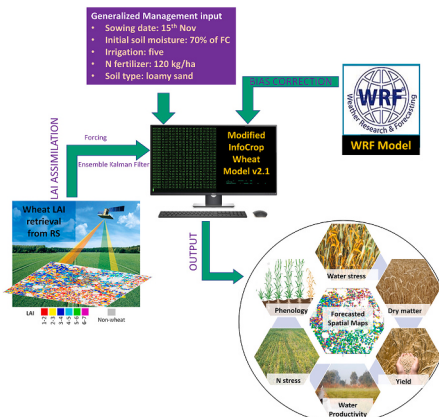
^e CCAFS, Borlaug Institute for South Asia, CIMMYT, India

^f Centre for Atmospheric Sciences, Indian Institute of Technology Delhi, New Delhi, India

HIGHLIGHTS

- Developed a prototype spatial wheat yield forecasting system assimilating remote sensing and weather forecast in crop simulation model
- Multidate remotely sensed leaf area index retrieved by inversion of canopy radiative transfer model was assimilated using Ensemble Kalman Filter
- Assimilation compensated for field-to-field variability in variety, sowing date and management practices even with uniform values specified to model
- Forecasted phenology, biomass and yield of wheat at field scale with good accuracy which improved with each date of data assimilation
- Prototype can be applied from field to region for crop insurance, agro-advisory, supply chain management, food security, resource allocation, etc.

GRAPHICAL ABSTRACT



ARTICLE INFO

Editors: Pytrik Reidsma and Van Snow

Keywords:

Prediction

Radiative transfer

ABSTRACT

CONTEXT: An accurate crop yield forecast with sufficient lead time is critical for various applications, such as crop management, resources mobilization, agri-commodity trading, crop insurance, etc. Accurate yield forecasting well ahead of harvest at field scale with minimal field input data remains a challenge.

* Corresponding author at: Division of Agricultural Physics, ICAR - Indian Agricultural Research Institute, New Delhi, India
E-mail address: vk.sehgal@icar.gov.in (V.K. Sehgal).

Crop phenology
Ensemble kalman filter
Data assimilation

OBJECTIVE: This study aimed to develop a novel prototype wheat yield forecasting system by assimilating remote sensing (RS) derived crop parameters and weather forecast into InfoCrop-Wheat crop simulation model (CSM), using minimum field measurements.

METHODS: The CSM was calibrated and validated at both research farm and farmers' fields. The crop LAI was retrieved through inversion of the PROSAIL radiative transfer model from Sentinel-2A and Landsat-8 images and validated using in-situ LAI measurements. The CSM was modified to test assimilation of RS derived LAI through "Ensemble Kalman Filtering" (EnKF) and "Forcing" strategies at multiple time-steps. The RS derived LAI was not only used to correct/replace model simulated LAI but other model state variables were also adjusted accordingly. A major challenge of adjusting crop phenology based on RS derived LAI was also attempted. The WRF weather forecast was bias-corrected and incorporated into the modified model-LAI assimilation framework. Generic crop management inputs were specified to the model. Finally, the study demonstrated a workable prototype of a field scale wheat growth and yield forecasting system under limited field data availability.

RESULTS AND CONCLUSIONS: The inversion of PROSAIL showed an RMSE of $0.56 \text{ m}^2/\text{m}^2$ in LAI retrievals. Model validation with measured inputs showed normalized error (NE) of 6–8% in grain yield. The proposed framework showed only 2%, 5%, 3% and 1% higher NE in simulating days to anthesis, days to physiological maturity, dry matter and grain yield, respectively, than with measured inputs. The "EnKF" outperformed "Forcing" for predicting crop yield as well as phenology and growth of wheat using generic management inputs. The system showed acceptable accuracy in forecasting phenology, dry matter and yield of wheat at field scale when weighted adaptive bias-correction of weather forecast was incorporated with a 15 days lead time.

SIGNIFICANCE: The prototype can be scaled-up for wheat and other crops for predicting real-time crop condition and yield losses at farmers' field for a range of applications, notably, crop-insurance, resources allocation, targeted agro-advisories and triggering contingency plans. It offers considerable potential for objective assessment of crops in the marginal and smallholder systems supporting the smart farming paradigm.

1. Introduction

Public and private players in market-driven agricultural economy demand an accurate and timely forecast of crop yields for the applications such as crop management, stocking food supply, strategic resource mobilization, trading, logistic, insurance and financial decision etc. (Fang et al., 2011; Pagani et al., 2019). Traditional yield forecasting methods rely on agro-meteorological models or spectral-agromet models, which suffers from the limitation of the site and crop/variety specificity (Doraiswamy et al., 2003). Crop simulation models (CSM) are been increasingly used to monitor crop growth and estimate yield. However, they have limitations of applicability at regional scale due to two main reasons: (1) non-availability of a large amount of input data on management practices at field scale, such as variety, sowing date, seed rate, fertilization rate and schedule, irrigation rate and schedule etc. as their collection for large area require labour, money and time, and (2) difficulty in validating modelling output at the regional scale. Therefore, forecasting yield or developing a crop growth monitoring system at a field scale over a region with minimal input data remains a significant challenge for researchers. This study aimed to address these issues by proposing and developing such a prototype system for wheat yield forecasting at the field scale.

Independently, remote sensing (RS) and CSM have certain advantages and disadvantages for crop growth monitoring and yield prediction application. RS technology provides real-time synoptic and repetitive coverage of a geographical area with information collection capabilities on a range of spatial scales. Thus, it is ideally suited for crop growth monitoring concerning abiotic stresses at regional scales and providing early warnings. RS has limitations in quantifying the absolute changes in crop biophysical parameters and crop yield losses. For effective monitoring, satellite observations are to be complemented with in-situ observations (of weather, soil, crops), ground survey and model outputs. In contrast, CSMs, which are used to monitor crop growth and estimate yields, have limitations in their application at regional scales. The limitations, at this scale, are linked to the difficulty of estimating some of the model input parameters and/or model initial conditions (Moulin, 1999). A combination of remotely sensed information and crop model is a promising approach that compliments the shortcomings of each of the tools to provide a technological solution for near real-time assessment of crop growth both qualitatively and quantitatively (Moulin et al., 1998). The basis of this RS-model coupling is that remotely

sensed measurements can be related to the instantaneous values of various canopy state variables (Sehgal et al., 2002). The canopy state variables can be connected to remotely sensed measurements by using physical radiative transfer models or empirical relationships (Dhakar et al., 2019b; Sehgal et al., 2016). The main advantage of using remotely sensed information is that it quantifies the actual state of the crop (over a large area) that are less labour and material intensive than in-situ sampling. On the other hand, CSMs provide a continuous estimate of crop growth for a field over a period (Delécolle et al., 1992). The added value of crop models and remote sensing is that both are objective, quantitative and consistent over large areas.

The application of crop simulation models for yield prediction before the harvest typically suffers from three kinds of uncertainties, viz. error in driving variables, intrinsic model errors, and error in the measured crop states. Error in driving variable (weather-related uncertainty) arises mainly because of less accurate seasonal forecast during the early season of crop growth but improves as the season's progresses when weather observation becomes available (Ines et al., 2013). Model related uncertainty is caused by the oversimplification of modelled processes, systematic errors in the model and errors in input data (Ines et al., 2013; Maas, 1988; Moulin et al., 1998). Weather-related uncertainty can potentially be minimized through the skillful forecast of driving variables, whereas model related uncertainty can be minimized by assimilating multiple remote sensing observations during the crop growing season (de Wit and van Diepen, 2007; Hansen et al., 2006; Ines et al., 2013; Vazifedoust et al., 2009).

Assimilation of remotely sensed state variables into CSMs has been accomplished by following various strategies of updating, forcing, and simulation steering (Bach and Mauser, 2003; Delécolle et al., 1992; Ines et al., 2013; Maas, 1988; Makowski et al., 2006; Moulin et al., 1998; Paniconi et al., 2003; Sehgal et al., 2002; Sehgal and Sastri, 2005). Forcing strategy is a special case of updating mechanism, in which remote sensing observation directly replaces the model state variable by assuming that remote sensing observations are free of error or level of data error is acceptable to be propagated within the simulated system. Many papers have reviewed the coupling of remote sensing observation and CSMs (Dorigo et al., 2007; Fischer et al., 1997; Jin et al., 2018). Algorithms for assimilating observations into models can be subdivided into four categories, viz., optimal interpolations, experimental methods, continuous methods and sequential methods. Of the algorithms, sequential data assimilation has been a widely used algorithm for

updating RS derived state variables into crop models (Bolten et al., 2010; Crow and Wood, 2003; de Wit and van Diepen, 2007; Hadria et al., 2006; Nearing et al., 2012). Compared to continuous assimilation, sequential data assimilation offers ease of implementation, computational efficiency, and optimum performance as it accounts for uncertainties in both observations and the model itself (Ines et al., 2013; Li and Bai, 2013). Moreover, sequential data assimilation can be implemented in CSM without changing the model structure.

The current sequential data assimilation includes the Kalman Filter (KF), Extended Kalman Filter, Ensemble Kalman Filter (EnKF) and Particle Filter (PF). These algorithms quantify relative weights between model-simulated state and observed state variable to minimize error propagation in further simulations sourced from either model or observation uncertainty. KFs (Kalman, 1960) are widely used as a sequential data assimilation strategy but have limitations while applying for agroecosystem models (McLaughlin, 2002). KFs can only be applied if the model is linear and the errors have a normal distribution. However, equations of dynamic crop simulation models are seldom linear for the state variables and the model parameters. KFs cannot deal with high dimensionality and threshold functions that are usually included in agroecosystem models (Dorigo et al., 2007). The complex structure of crop models does not allow KFs to be formulated very well into a state-space equation. KFs are also unable to cope with model-related uncertainty. To address these issues with KFs, Evensen (2003) developed the Ensemble Kalman Filter.

Several studies have shown the robustness of EnKF to assimilate RS observations in hydrological and meteorological models with substantial success (Crow and Wood, 2003; Das et al., 2008; Dunne and Entekhabi, 2005; Evensen, 2003; Keppenne and Rienecker, 2002; Reichle et al., 2002). EnKF has recently been used with crop models with some success and challenges, especially when assimilating leaf area index (LAI) (Curnel et al., 2011). Remotely sensed data such as soil moisture (Ines et al., 2013; van Loon and Troch, 2002), LAI (Dente et al., 2008), and evapotranspiration (ET) (Kamble et al., 2013; Vazifedoust et al., 2009) were satisfactorily assimilated into agro-hydrological models using EnKF.

LAI is the most widely assimilated variable in CSMs because of (a) its crucial roles in various physiological processes such as light interception and gas exchange indicating crop growth condition, showing the comprehensive effects of management and growing environment, and determining the biomass and yield in crop model (Curnel et al., 2011; de Wit and van Diepen, 2007; Huang et al., 2016; Ma et al., 2013; Maas, 1988; Mokhtari et al., 2018; Zhao et al., 2013; Sehgal et al., 2002), and (b) its robust estimation from the multi-spectral remote sensing data (Dhakar et al., 2019b; Sehgal et al., 2016).

For these tools to forecast crop yield, it is important to assimilate extended-range weather forecasts along with remote sensing inputs into a CSM. Integration of weather forecast and CSM potentially can add value to in-season crop yield forecasting but is limited by the non-availability of an accurate real-time weather forecast and input weather variables that are compatible with CSMs (Togliatti et al., 2017). Therefore, a combination of historical and current weather data is used for crop yield forecasting through CSM in various regions such as Europe (Williams and Falloon, 2015), Australia (Carberry et al., 2009), Canada (Chipanshi et al., 2015), Nebraska-USA (Morell et al., 2016) and Iowa-USA (Archontoulis et al., 2016). Very few studies have used combinations of historical, current and forecasted weather data from dynamical climate models for in-season crop yield forecasting (Archontoulis et al., 2016; Togliatti et al., 2017). Studies combining weather forecast and crop models also differ on the use of many weather variables for simulations; very few weather forecasting models provide the solar radiation which can be directly used in crop models. These include the National Digital Forecast Database (NDFD; 4-day forecast), the Climate Forecast System (CFS; 6-months forecast), and the Weather Research and Forecasting model (WRF) that can be run for different forecast lengths of one's choice. So, strategies exist to assimilate remote sensing data into

crop simulation models and weather forecasts from dynamic weather models for crop forecasting but have not been demonstrated and validated together as an application.

Among the various CSMs, InfoCrop-wheat v2.1 model was used (Aggarwal et al., 2006). Firstly, the CSM performance was evaluated at an experimental research farm and farmers' fields. Secondly, the model state variable LAI was chosen as the coupling parameter of the crop model and derived from remote sensing observations. A validated strategy of LAI retrieval from LANDSAT operational land imager (OLI) and Sentinel-2A multispectral imager (MSI) imagery by inversion of radiative transfer model was followed (Dhakar et al., 2019b). Thirdly, weather forecast at a finer scale was generated using the WRF model (Skamarock et al., 2016). Lastly, a novel regional wheat yield forecasting framework was developed by assimilating remote sensing derived LAI and weather forecast into a crop model for spatial yield forecasting of wheat, addressing various challenges, described in the following sections.

2. Materials and methods

2.1. Study area

To evaluate the proposed wheat yield forecasting prototype system, the study was conducted over farmers' fields situated in Pataudi block of Gurugram district, Haryana, India, during two winter seasons (November to April) of 2015–16 and 2016–17 (Fig. 1). Farmer's fields were selected to capture the range in field sizes, sowing dates and management practices followed. The details of the study area can be found in our published study (Dhakar et al., 2019b). The data on management practices, leaf area index, biomass and grain yield were collected from each selected farmers' field. Forty wheat fields (20 fields in each year) were selected for conducting the study. None of the fields was less than 900 m², while more than 50% were 4000 m² or more in area. Wheat LAI was measured (five replications per field) at different dates during the crop season, synchronizing with satellite passes. The biomass and yield were sampled from a 2 × 2 m² area (three replication per field) at the harvest.

2.2. Development of prototype

This study attempted to develop a novel prototype of a wheat yield forecasting system by integrating remotely sensed LAI and weather forecast into the CSM multiple time during the crop season. Following steps were followed to develop the prototype system, and an overall methodological flow chart is presented in Fig. 2.

1. Retrieval of LAI from remotely sensed data through inversion of the PROSAIL model (Jacquemoud et al., 2009).
2. Development of modified InfoCrop-LAI assimilation sub-module.
3. Simulation experiments using standard uniform management practices for testing and validation of modified InfoCrop-LAI model.
4. Generation of weather forecast using the WRF model at an interval of 15 days.
5. Adaptive bias correction of the weather forecast.
6. Assimilation of bias-corrected weather forecast into modified InfoCrop-LAI model.
7. Implementation of prototype to generate crop growth and yield forecast maps.

3. Step-1: Retrieval of LAI using remotely sensed data through inversion of PROSAIL model

Landsat-8 operational land imager (OLI) having 30 m spatial resolution and Sentinel-2 multi-spectral imager (MSI) having 20 m spatial resolution images were used in this study (Table 1). LAI was retrieved at three dates during the 2015–16 and 2016–17 crop seasons. The

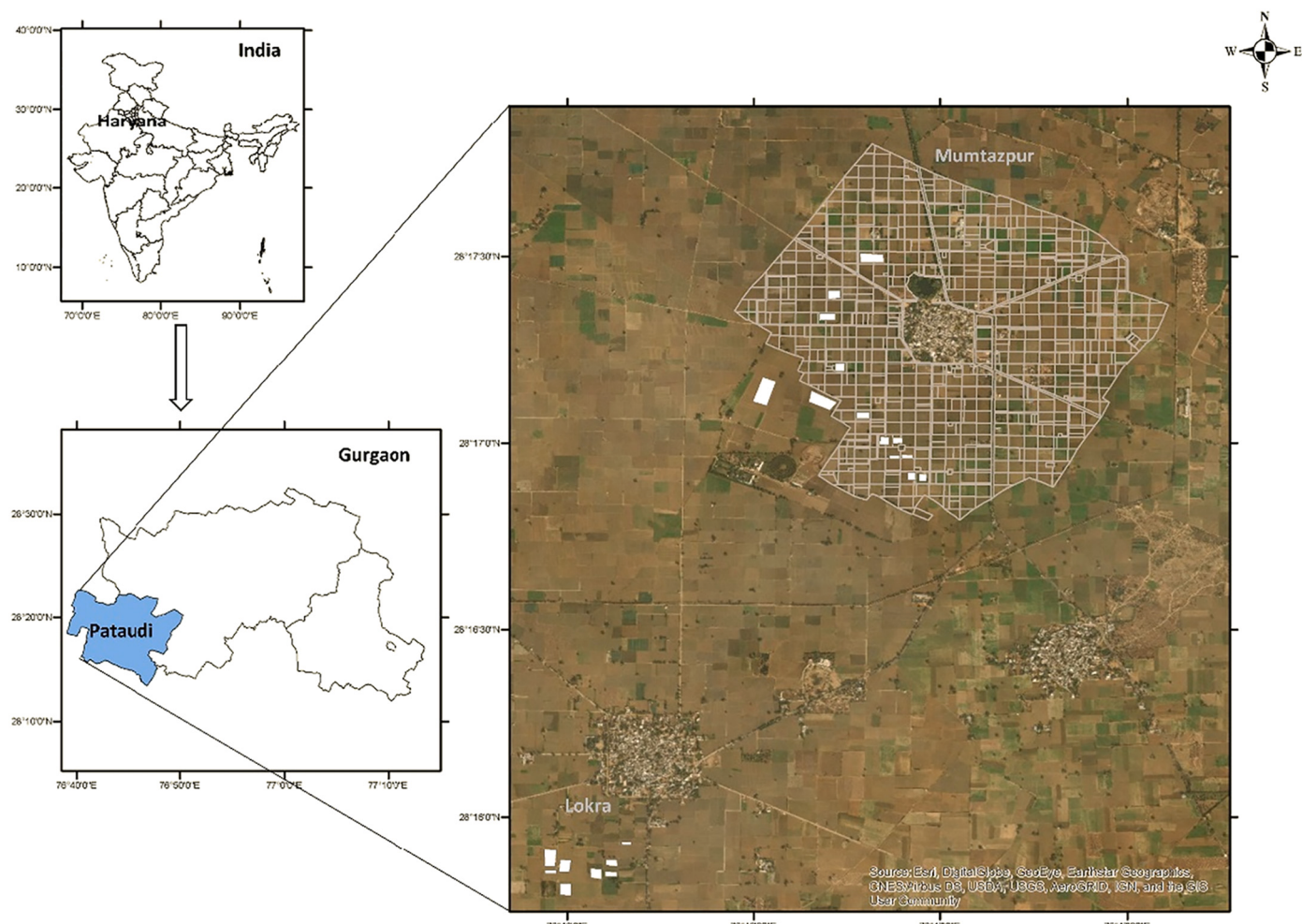


Fig. 1. Study area showing selected fields (white filled) overlaid on a satellite image.

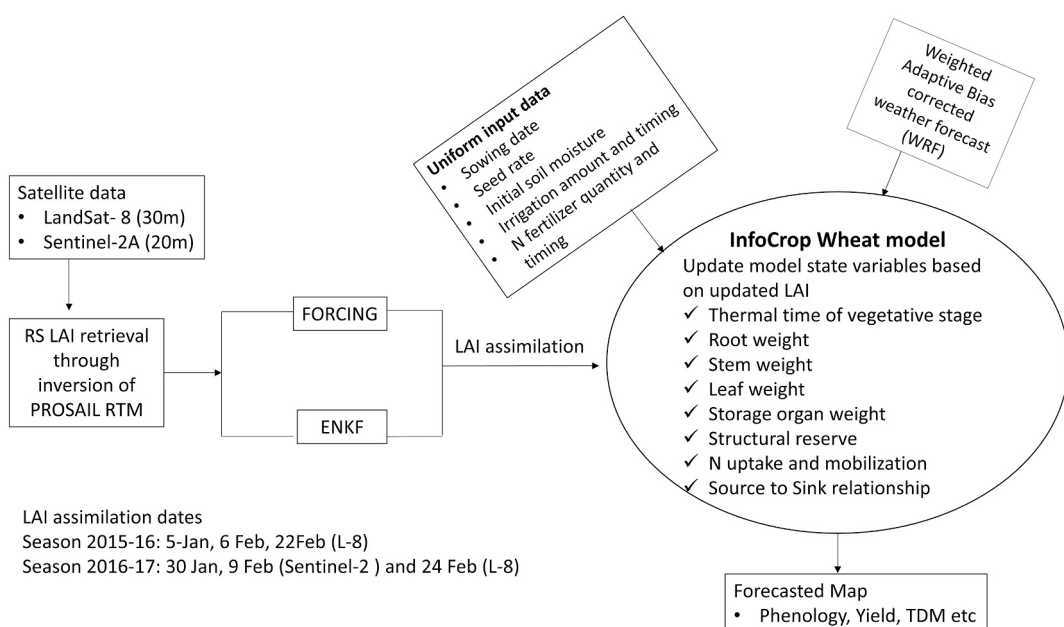


Fig. 2. Overall methodology framework.

Table 1

Remote sensing dataset used in this study.

Satellite	Sensor	Acquisition date	Product	WRS Path/Row* or Tile number	Spatial resolution
Landsat - 8	OLI (Operational Land Imager)	5-Jan-2016 8-Feb-2016 22-Feb-2016 24-Feb-2017	L1TP (Quantized and calibrated scaled Digital Numbers (DN))	147/40	30 m
Sentinel – 2A	MSI (Multi-spectral Instrument)	30-Jan-2017 9-Feb-2017	L1C (top-of-atmosphere reflectances in cartographic geometry)	T43RFM	Resampled at 30 m

* for Landsat; #for Sentinel.

extensively used canopy radiative transfer (RTM) model PROSAIL-5B (Dhakar et al., 2019b; Huang et al., 2019; Jacquemoud et al., 2009; Lunagaria and Patel, 2019) was employed in this study for LAI retrieval. The LAI was retrieved through the look-up-table (LUT) approach after atmospheric correction of images by FLAASH™ (ENVI, 2009), which is a GUI application based on MODTRAN 4 atmospheric radiative transfer model. The details of the methodology of LAI retrieval and its validation are given in Dhakar et al. (2019b) and Sehgal et al. (2016). The LAI retrievals were validated with in-situ measurements collected over the two seasons.

4. Step-2: Development of modified InfoCrop-LAI assimilation submodule

4.1. InfoCrop model description, parameterization and validation at farmers' field

InfoCrop is a generic CSM that simulates the effect of genotype, weather, agronomic management, water, nitrogen, carbon and pests on the growth, development and yield of the crops in tropical agro-environments and its details are given in Aggarwal et al. (2006). Model parameterization was done based on the field experiments conducted at the farm of Indian Agricultural Research Institute, New Delhi (coordinates 28°38'23"N, 77°09'27"E) during the winter season of 2015–16 and 2016–17 (Dhakar et al., 2021). The details of model parameterization and validation at farmers' fields are elaborated in our other study (Dhakar et al., 2019a).

4.2. LAI assimilation strategies into the CSM

Leaf area index (LAI) was chosen as a coupling variable for linking remote sensing input into the InfoCrop-wheat model as it is a critical model state variable and can be retrieved from remote sensing. In this study, two assimilation strategies viz., Forcing and Ensemble Kalman Filter (EnKF), were employed for updating the LAI into the CSM at the time steps when LAI measurements are available during the crop season. InfoCrop-wheat model's source code was modified for incorporating the assimilation strategies. The two simulation switch variables of "FORCING" and "ENKF" were incorporated to choose between the 'assimilation' and 'no assimilation' run of the model. The two switches could have the following settings:

- When FORCING = 0.0 and ENKF = 0.0, then LAI will not be assimilated into the crop model (Open-loop simulations)
- When FORCING = 1.0 and ENKF = 0.0, then LAI will be assimilated into the crop model by Forcing strategy (Forcing simulation)
- When FORCING = 0.0 and ENKF = 1.0, then LAI will be assimilated into crop model by ensemble Kalman filter strategy (EnKF simulations)
- When FORCING = 1.0 and ENKF = 1.0, then the model will report an error.

In the "Forcing" strategy, the model simulated LAI was updated with measured LAI values on different days. The measured LAI was forced

one day at a time and so the state variable's updated value determined the values of rate and state variables at the next time step, steering the model on a correct path.

The 'EnKF' strategy updated not only a state variable (LAI) but also updated specific leaf area (SLAVAR, unit: $\text{dm}^2 \text{ mg}^{-1}$), a model parameter. The SLAVAR is updated once at the first-time step of assimilation to fine-tune this genetic coefficient which is characteristic of a genotype/variety. As with other management inputs, we may not be knowing the wheat variety grown in the field. So, the generic SLAVAR value is adjusted once, at first assimilation, so that we can account for some differences in wheat varieties grown in the fields. The 'EnKF' algorithm was implemented in the following steps:

- (1) Generate an ensemble of N values ($N = 40$ in this case) of parameter SLAVAR by following the normal distribution $N(\mu_{\text{SLAVAR}}, \sigma^2_{\text{SLAVAR}})$ with values expressed as $\{\text{SLAVAR}^1, \dots, \text{SLAVAR}^j, \dots, \text{SLAVAR}^N\}$, where ' j ' is the element of N ensembles ($j = 1, \dots, N$). The value of μ_{SLAVAR} and σ^2_{SLAVAR} was obtained as $0.0023 \text{ dm}^2 \text{ mg}^{-1}$ and $0.0101 (\text{dm}^2 \text{ mg}^{-1})^2$ from field experimentation, respectively.
- (2) Generate an ensemble of N values of the error term $\varepsilon_{T,i}^j \sim N(0, Q)$ where Q is the model variance, T is the day of the i^{th} observation ($i = 1, 2, 3$). The Q was taken as constant ($Q = 0.12$ (dimensionless for LAI)) determined from the field experiment.
- (3) Generate an ensemble of N values of the state variable (LAI) using model equation

$$\text{LAI}_{T,i}^j = \text{WLVI} * \text{SLAVAR}_{T,i}^j * \text{AFGEN}(\text{SLACF}, \text{DSI}) + \text{GLAI}_{T,i}^j - \text{DLAI} + \varepsilon_{T,i}^j \quad (1)$$

Where, WLVI is initial leaf weight, SLACF is the function of developmental stage (DSI), GLAI is the leaf area growth rate, DLAI is the death rate of LAI and AFGEN is a linear interpolation function.

- (4) Compute the (2×2) variance-covariance (Δ) matrix from the N ensembles of model LAI and SLAVAR

$$\Delta = \begin{bmatrix} \text{var}(\text{LAI}_{T,i}^j) & \text{cov}(\text{LAI}_{T,i}^j, \text{SLAVAR}^j) \\ \text{cov}(\text{LAI}_{T,i}^j, \text{SLAVAR}^j) & \text{var}(\text{SLAVAR}^j) \end{bmatrix} \quad (2)$$

- (5) Compute the Kalman Gain (KG) for state variable (LAI) and model parameter (SLAVAR) on the day of measurement

$$KG_{\text{LAI}} = \frac{\text{var}(\text{LAI}_{T,i}^j)}{\text{var}(\text{LAI}_{T,i}^j) + \text{var}(\text{MLAI})} \quad (3)$$

$$KG_{\text{SLAVAR}} = \frac{\text{cov}(\text{LAI}_{T,i}^j, \text{SLAVAR}^j)}{\text{var}(\text{LAI}_{T,i}^j) + \text{var}(\text{MLAI})} \quad (4)$$

Where, var(MLAI) is the variance of measurement error in LAI; if var(MLAI) = 0, we assume no error in measurement of the state

variable but this assumption is rarely valid and often measurement error is substantial. If the measurement has a significant variance compared to the model variance, one gives more weight to the model simulation and vice-versa.

- (6) Generate an ensemble of N observations of LAI ($LAI_{OBS}^1, i, \dots, LAI_{OBS}^N, i$) by following a normal distribution $N(LAI_{OBS}, var(MLAI))$ where LAI_{OBS} is measured LAI.

- (7) Update the state variable (LAI) using Kalman gain

$$LAI_{NEW}^j = LAI_{T,i}^j + KG_{LAI} * (LAI_{OBS}^j - LAI_{T,i}^j) \quad (5)$$

$$\overline{LAI_{NEW}} = \frac{\sum_{j=1}^N LAI_{NEW}^j}{N} \quad (6)$$

Where, $\overline{LAI_{NEW}}$ is the updated mean value of LAI and used at the next time step of model simulation to steer the model on the correct path.

4.3. Updating other model state variables

Once the LAI is updated at a given time step by either 'Forcing' or 'EnKF' strategy, it was followed by updating other state variables at subsequent time steps to steer the model on a correct simulation path. It was observed that the model became unstable and showed unpredictable behavior when only a single state variable (i.e. LAI) is updated. It may be due to the fact that unless all model state variables are updated on the day of observation in sync, the model may show inconsistencies in simulation (Maas, 1988). The inconsistencies in simulation may arise because there can't be entirely disproportionate growth of different plant organs viz., root, stem, leaves and storage organs at a given time step in dynamic CSM. Thus, some strategy was needed for updating the other state variables along with LAI.

To update other state variables, a correction factor (CF) was computed as the ratio of observed LAI (i.e. remotely sensed LAI) and simulated LAI and was multiplied with the simulated value of other state variables to adjust them in proportion to change in LAI (Sehgal et al., 2002). Dry matter production of plant organs like green leaf weight (WLVG), stem weight (WST), root weight (WRT), storage organ weight (WSO) and non-structural reserve weight (WIR) were adjusted in the proportion of LAI change based on the correction factor. Updating of WSO was permitted only if the day of LAI assimilation occurred after the anthesis stage. In the source-sink balance module, the number of storage organs per day was also adjusted by CF and was allowed only during the post-anthesis stage. The crop N-uptake was also updated by altering the crop N-demand of different plant organs viz., leaves (NDELV), stem (NDEMST), root (NDEMRT) and storage organ (NDEMSO). The actual N-content of different organs ANLV (leaves), ANST (stem), ANRT (root) and ANSO (storage organ) were also adjusted based on the CF to maintain the nitrogen balance.

Besides adjusting other state variables, it was necessary to adjust the crop phenology in the model based on the remote sensing observations to account for variations in growth due to early and late sowing compared to normal sowing. It was observed that LAI assimilation without phenology correction led to unusual high total dry matter and yield in the late sown crop resulting in significant error in simulation. Adjustment of phenology based on LAI assimilation in this study is a novel concept. It was accomplished by modifying the thermal time requirement (TTVG) for emergence to anthesis stage based on the LAI assimilation at the first time-step. The first date of LAI assimilation must therefore be before the median anthesis time of wheat crop in the study region for this algorithm to work. We hypothesized that the relationship between thermal time requirement and LAI of a crop sown during different sowing windows is unique in a given region. A crop sown before the median sowing date will require more thermal time and vice-

versa (i.e. the crop sown after the median sowing date will require less thermal time). Therefore, we developed a relation between LAI and thermal time requirement as a function of the developmental stage. The relation was captured in terms of the LAITHERM variable (i.e. slope of regression line) by running the simulation model for different sowing dates under potential production (i.e. no water and nitrogen limitation) (Fig. 3). The thermal time requirement is also controlled by the first date of LAI assimilation (DOA- in terms of days after sowing) and median anthesis date (REFANTHD - in terms of days after sowing). Thus, the modified thermal time requirement (TTVGM) was calculated as:

$$TTVGM = TTVG + (LAI_A - LAI_M) * LAITHERM * \frac{REFANTHD}{REFANTHD - DOA} \quad (7)$$

Where, LAI_A is assimilated LAI and LAI_M is model simulated LAI.

4.4. Sensitivity of modified InfoCrop-LAI assimilation framework

To assess the sensitivity of the modified InfoCrop-LAI assimilation framework, various hypothetical scenarios of crop growth (in terms of LAI) with markedly varying LAI at 50, 80 and 100 days after sowing (DAS) were designed, and their effect on simulations of phenology, total dry matter and yield were investigated. The results are elaborated along with details of LAI assimilation scenarios in supplementary material section 1.3 and Table S1.

5. Step-3: Simulation experiments using standard crop management practices for testing and validation

One of the significant limitations of the application of CSM on a regional scale is the non-availability of initial conditions, variety sown, and management practices followed in different fields in the region. So, the proposed modified InfoCrop-LAI assimilation framework was tested for the farmers' fields, assuming that all fields were exposed to the same weather conditions, having the same soil profile, initial conditions and with the same variety and sowing time followed as per standard uniform management practices. This deliberately entailed errors in field-to-field model simulation mimicking the situation of unavailability of model inputs. Then we evaluated how the assimilation of LAI and adjustment of other state variables and phenology were able to correct for these errors.

Standard uniform inputs specified were:

- **Weather:** We used weather data from the only automatic weather station installed at Krishi Vigyan Kendra, Sikohpur (28.37° N latitude; 76.98° E longitude) as all the selected fields were in the 10-km periphery of the weather station. So, no field-to-field variability in the weather was specified in the model.
- **Soil:** We specified the dominant soil profile present in the study region which is loamy sand in texture. The soil profile was simulated in three layers, i.e. 300, 600, 600 mm of thickness, resulting in a profile

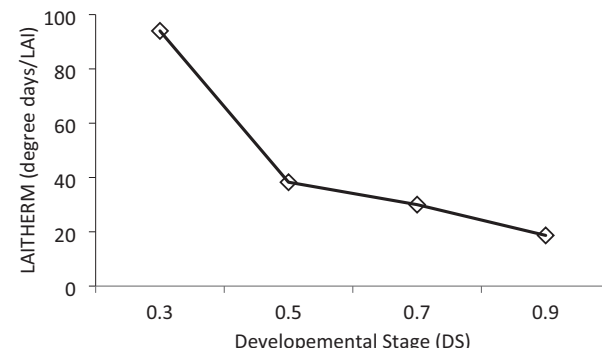


Fig. 3. The LAITHERM (slope of the relation between thermal time requirement and LAI) as a function of developmental stages.

depth of 1500 mm. Soil parameters in the InfoCrop model consist of layer-wise soil texture (% Sand, % Silt and % Clay), soil bulk density, soil organic carbon, soil saturated hydraulic conductivity, soil water holding capacity, soil permanent wilting point and soil moisture saturation content. Other soil parameters were soil electrical conductivity, soil pH and slope. The model was given the same value for all the soil parameters for each of the farmers' fields.

- **Sowing date (DOS):** Specified 15th November as the sowing date for all the farmers' fields, which is the recommended regular sowing date in the study area (Kumar et al., 2014).
- **Fertilizer amount & schedule:** Recommended nitrogen fertilizer application rate of 120 kg/ha in three split doses of 60, 30, 30 kg/ha at 0, 21, 40 days after sowing, respectively, as specified for all the farmers' fields.
- **Irrigation amount & schedule:** Fixed five number of irrigations each of 50 mm was applied at 20, 40, 60, 80, 100 days after sowing as per recommended practice for all the farmers' fields.
- **Seed rate:** Recommended seed rate of 100 kg/ha was specified for all the farmers' fields.
- **Initial soil moisture:** Simulations were started 20 days before sowing to initialize the soil water balance. Initial soil moisture was uniformly kept at 70% of moisture content at the field capacity of the soil as is practiced by farmers in the area.

Evapotranspiration was modelled using the modified Penman-Monteith formula. Eighteen simulation experiments were designed using a combination of measured inputs, standard inputs and assimilation strategies (Table 2). Validation of output was carried out in terms of root mean square error (RMSE) and normalized RMSE (nRMSE) between simulated and observed values for different farmers' fields.

6. Step-4: Generation of weather forecast using WRF model

WRF model (Skamarock et al., 2016) version 3.8.1 was set up to generate the weather forecast at different time scales in hindcast mode. The Advanced Research WRF (ARW) core was used for generating the weather forecast. Three-way nesting was implemented for defining the

Table 2

Simulation experiments on LAI assimilations using standard uniform inputs for the selected farmers' fields.

Exp. No.	Season	Management inputs	LAI assimilation	Phenology adjustment
1	2015–16	Standard uniform inputs except measured DOS	Forcing	No
2	2016–17	Standard uniform inputs except measured DOS	Forcing	No
3	2015–16	Standard uniform inputs except measured DOS	EnKF	No
4	2016–17	Standard uniform inputs except measured DOS	EnKF	No
5	2015–16	Standard uniform inputs	Forcing	No
6	2016–17	Standard uniform inputs	Forcing	No
7	2015–16	Standard uniform inputs	EnKF	No
8	2016–17	Standard uniform inputs	EnKF	No
9	2015–16	Standard uniform inputs	Forcing	Yes
10	2016–17	Standard uniform inputs	Forcing	Yes
11	2015–16	Standard uniform inputs	EnKF	Yes
12	2016–17	Standard uniform inputs	EnKF	Yes
13	2015–16	Standard uniform inputs	Open-loop	Yes
14	2016–17	Standard uniform inputs	Open-loop	Yes
15	2015–16	Standard uniform inputs	Open-loop	No
16	2016–17	Standard uniform inputs	Open-loop	No
17	2015–16	Standard uniform inputs except measured DOS	Open-loop	No
18	2016–17	Standard uniform inputs measured DOS	Open-loop	No

Measured DOS: date of sowing data collected from farmers' fields.

Open-loop: means no assimilation of LAI.

model simulation with the reference (central) location of our study area. Parent_grid_ratio for three domains were kept as 1:3:3 starting from the inner-most domain. The inner-most child domain (i.e. study area) was set as 100 × 100 km in size with a horizontal grid resolution of 1 km. The methodology for generating weather forecasts is further detailed in section 1.1 of the supplementary material.

7. Step-5: Weighted adaptive bias correction of the weather forecast

The weather forecasts are not free from errors. Therefore, the daily weather forecast from the WRF model except for rainfall was bias-corrected at 15 days lead time using an adaptive approach as follows:

$$\text{Adaptive bias correction} = \left(\sum_{i=1}^{i=15} (O_i - F_i) * W_i \right) + O_{i=0} \quad (8)$$

Where, O is observed weather, F is WRF forecasted weather, i is i^{th} day lead time, and W is weightage associated with i^{th} lead time. In non-weighted adaptive bias correction, we assumed uniform weightage ($W = 1$) over lead times. Whereas, in the case of weighted adaptive bias correction, we followed a logarithmic function for the weightage over 15 days lead time. So, the smaller lead time values were given a higher weight and longer lead time values were given a small weight following the logarithmic function. The logarithmic weighting function is provided in the supplementary material Fig. S1.

8. Step-6: Assimilation of bias-corrected weather forecast along with LAI into the crop model

To run the framework in forecasting mode, the weather files for the simulation model contained observed weather up to the date of weather

Table 3

Scenarios of progressive LAI assimilations along with either actual weather (AW) or bias-corrected weather forecast (WF).

Season	Simulation scenario	Period of actual weather used	Period of forecasted weather used
2015–16	LAI1 + AW	1-Nov-2015 to physiological maturity	Nil
	LAI2 + AW	1-Nov-2015 to physiological maturity	Nil
	LAI3 + AW	1-Nov-2015 to physiological maturity	Nil
	LAI1 + WF	1-Nov-2015 to 5-Jan-2016 (1st date of LAI assimilation)	6-Jan-2016 to physiological maturity
	LAI2 + WF	1-Nov-2015 to 6-Feb-2016 (2nd date of LAI assimilation)	7-Feb-2016 to physiological maturity
	LAI3 + WF	1-Nov-2015 to 22-Feb-2016 (3rd date of LAI assimilation)	23-Feb-2016 to physiological maturity
	2016–17	LAI1 + AW	1-Nov-2016 to physiological maturity
		LAI2 + AW	1-Nov-2016 to physiological maturity
		LAI3 + AW	1-Nov-2016 to physiological maturity
		LAI1 + WF	1-Nov-2016 to 30-Jan-2017 (1st date of LAI assimilation)
		LAI2 + WF	1-Nov-2016 to 9-Feb-2016 (2nd date of LAI assimilation)
	LAI3 + WF	1-Nov-2016 to 24-Feb-2016 (3rd date of LAI assimilation)	25-Feb-2016 to physiological maturity

LAI1: LAI assimilation on first date; LAI2: LAI assimilation on first and second date; LAI3: LAI assimilation on first, second and third date; AW: actual weather; WF: forecasted weather.

forecast followed by a bias-corrected forecasted weather data at 15 days lead time. The six sets of weather data scenarios were tested for each year corresponding to progressive LAI assimilation and are given in Table 3. Only LAI assimilation by EnKF strategy was employed for testing different weather scenarios as its performance was better than Forcing. The model performance for the six scenarios was validated in terms of yield, biomass and phenology.

9. Step-7: Generation of growth and yield forecast maps

The model was run for each pixel in the study area image for the two seasons under each of the scenarios given in Table 3. The maps of model output variables of days to anthesis, days to physiological maturity, biomass and yield were generated.

10. Statistical analysis

Standard statistical parameters of coefficient of determination (R^2), root mean square error (RMSE) (Eq. 9), normalized RMSE (nRMSE) (Eq. 10) and D-index (Eq. 11) were used to evaluate the LAI retrieval accuracy, performance of modified InfoCrop-LAI assimilation framework and modified InfoCrop-LAI assimilation-weather forecast framework. All these parameters were calculated for the whole growing season.

$$RMSE = \sqrt{\frac{\sum_{i=1}^n (O_i - P_i)^2}{n}} \quad (9)$$

$$nRMSE (\%) = \frac{RMSE}{\bar{O}} * 100 \quad (10)$$

The D-index was developed by (Willmott, 1981) and is a standardized measure of the degree of model prediction error and varies between 0 and 1. A value of 1 indicates a perfect match, and 0 indicates no agreement at all. It is calculated as:

$$D\text{-index} = 1 - \frac{\sum_{i=1}^n (P_i - O_i)^2}{\sum_{i=1}^n (|P_i - \bar{O}_i| + |O_i - \bar{O}_i|)^2} \quad (11)$$

Where, O_i = i^{th} observation, P_i = i^{th} predicted/forecasted value, \bar{O} = average of observed values and n = number of observations.

The accuracy of bias correction of weather forecast was evaluated using Pearson's correlation coefficient (r), RMSE, mean systematic bias (MSB) (Eq. 12) and mean absolute error (MAE) (Eq. 13).

$$MSB = \frac{\sum_{i=1}^n (P_i - O_i)}{n} \quad (12)$$

$$MAE = \frac{\sum_{i=1}^n |(P_i - O_i)|}{n} \quad (13)$$

11. Results

11.1. LAI retrieval accuracy

Wheat LAI retrieval through LUT based PROSAIL inversion was validated using in-situ measured LAI, and results are presented as a scatter plot in Fig. 4. It clearly shows that LUT based inversion of PROSAIL captured well the variability in LAI (0.4 to 5.8) over the season. Overall, the RMSE of LAI retrieval over the two seasons was 0.56 m^2/m^2 . Good agreement between observed and retrieved LAI was also achieved, as evidenced by the high coefficient of determination value ($R^2 = 0.78$), significant at $p < 0.001$.

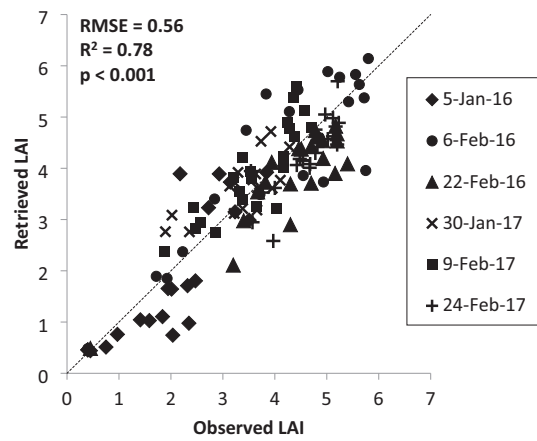


Fig. 4. Scatter plot between observed and retrieved wheat LAI on different dates over the two seasons.

11.2. Model validation at farmers' field with measured management inputs

InfoCrop model performance in simulating phenology, LAI, total dry matter and grain yield of wheat at selected farmers' fields by inputting actual management in the model is summarized in Table 4. The details of model validation results can be seen in our published study (Dhakar et al., 2019a). The results showed that the InfoCrop model could simulate the phenology, i.e. days to anthesis and physiological maturity, within the reasonable error of 3% and also achieved a good agreement between observed and simulated yield as is evident from high D-index values. The model showed an RMSE of 0.48–0.49 in LAI with a D-index of 0.94–0.95. The RMSE of mean total dry matter was about 600 kg/ha, and nRMSE was 4 to 5%. Grain yield also showed a good agreement, and errors were within the acceptable limit of 10%.

11.3. LAI assimilation with standard uniform inputs

Simulation experiments under standard uniform management practices with LAI assimilation as described in Table 2 were evaluated for days to anthesis and physiological maturity, total dry matter and grain yield of wheat for all the selected farmer's fields over the two seasons.

11.3.1. Days to anthesis and physiological maturity

Simulation experiments without LAI assimilation with standard uniform inputs (Exp. 15 & 16, i.e. reference experiments or control experiments) resulted in RMSE of about 8 to 10 days in the occurrence of anthesis and physiological maturity (Fig. 5a-b). Errors in the occurrence of anthesis and physiological maturity further increased when LAI was

Table 4

Summary of InfoCrop-wheat model validation at farmers' fields during season 2015–16 and 2016–17.

Parameter	2015–16			2016–17		
	RMSE	nRMSE (%)	D-index	RMSE	nRMSE (%)	D-index
Days to anthesis	2.91	3	0.85	2.89	3	0.93
Days to physiological maturity	2.38	2	0.98	2.72	2	0.98
LAI	0.48	13	0.95	0.49	13	0.94
Total dry matter (kg/ha)	602	5	0.88	593	4	0.94
Grain yield (kg/ha)	394	8	0.90	328	6	0.96

RMSE – root mean squared error; nRMSE – normalized RMSE; D-index – index of agreement.

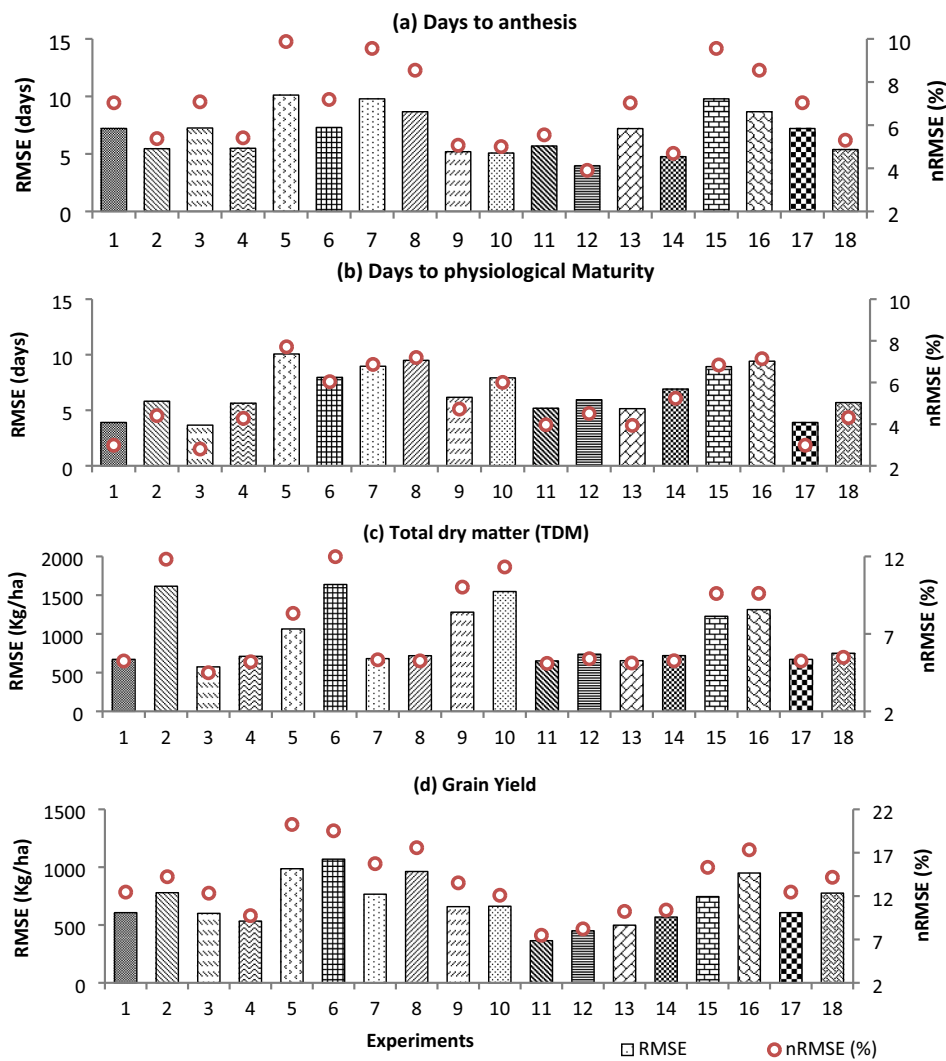


Fig. 5. Evaluation of modified model-LAI assimilation framework for simulating (a) days to anthesis, (b) days to physiological maturity, (c) total dry matter and (d) grain yield. The RMSE is the root mean squared error, and nRMSE is the normalized RMSE. The details of the experiments are provided in Table 2.

assimilated through Forcing without phenology adjustment with standard uniform inputs (Exp. 5). Simulation experiments without LAI assimilation and with standard uniform inputs except for the measured date of sowing (Exp. 17 & 18) reduced the nRMSE by 3 to 4% over control in anthesis and physiological maturity durations. Similar error reduction was also observed in the simulation experiments with LAI assimilation (either through Forcing or EnKF) and standard uniform inputs except for the measured date of sowing (Exp. 1 to 4). Phenology adjustment based on first LAI assimilation (Exp. 13 & 14) also reduced error similar to that in Exp. 17 & 18. It showed that the measured date of sowing could be replaced with modification in the model for phenology adjustment based on LAI assimilation. The least error in anthesis and physiological maturity timing was achieved when LAI was assimilated through EnKF with phenology adjustment (Exp. 12).

11.3.2. Total dry matter

Reference experiments showed RMSE of ~1200–1300 kg/ha in the total dry matter, equivalent to 10% nRMSE (Fig. 5c). Error in the total dry matter further increased when LAI was assimilated through Forcing with standard inputs, especially during the 2016–17 season (Exp. 2, 6, 9 & 10). Simulation experiments without LAI assimilation and with standard inputs except for the measured date of sowing (Exp. 17 & 18) resulted in ~4.3% reduction in normalized error in the dry matter over that of reference experiments. Similar error reduction was also observed

in the simulation experiments with only phenology adjustment based on first LAI assimilation (Exp. 13–14). Further appreciable decrease in total dry matter error was not achieved by LAI assimilation through EnKF (Exp. 12). Results imply that the measured date of sowing can be replaced by modifying the model for phenology adjustment based on LAI assimilation

11.3.3. Grain yield

Reference experiments showed RMSE of ~745–950 kg/ha days in grain yield, equivalent to 15–17% nRMSE (Fig. 5d). LAI assimilation without phenology adjustment resulted in the highest error in grain yield and was more in the case of Forcing (RMSE ~986–1086 kg/ha and nRMSE ~20%) than in EnKF (RMSE ~766–962 kg/ha & nRMSE ~16–17%). Phenology adjustment alone resulted in about a 5% reduction in normalized error over the reference experiments. LAI assimilation through Forcing along with the measured date of sowing could reduce error by 3% only as compared to reference experiments while it was about 4% in the case of EnKF. Lower error in grain yield (RMSE ~360–450 kg/ha & nRMSE ~7–8%) was achieved when LAI was assimilated through EnKF and phenology was adjusted based on first LAI assimilation (Exp. 11–12). Detailed results on observed versus simulated days to anthesis, days to physiological maturity, total dry matter and grain yield along the 1:1 line under different simulation experiments are provided in supplementary material section 2.1

11.4. Forecast verification and bias correction of the weather forecast

Forecasted weather from WRF model was verified using station data to determine the accuracy of the deterministic forecast for the wheat-growing period. Systematic biases in the forecast were corrected using non-weighted and weighted adaptive bias correction methods. The verification measures of RMSE, MAE, correlation coefficient (*r*), and MSB are provided in Table 5. Weighted adaptive bias correction significantly reduced the errors in weather forecast than non-weighted adaptive bias correction. Therefore, grid-wise WRF modelled weather forecast was corrected by weighted adaptive bias correction for its further use in the CSM. The detailed results on bias correction of weather forecast are given in supplementary material section 2.2.

11.5. Evaluation of modified Infocrop-LAI assimilation-weather forecast framework

Weighted adaptive bias corrected weather forecast was incorporated into the modified InfoCrop model-LAI assimilation framework. In this system, LAI was assimilated through EnKF only because it resulted in a lower error in simulated parameters. The performance of this forecasting system was evaluated in terms of nRMSE for the days to anthesis and physiological maturity, total dry matter and grain yield of wheat (Fig. 6). Six scenarios for each season were designed with the combination of three dates of LAI assimilation, actual weather (AW) and bias-corrected weather forecast (WF) as described in Table 3.

Results showed that the error in simulating days to anthesis was more in 2015–16 (nRMSE ~6%) than that in 2016–17 (nRMSE ~3.6%). The error in simulating days to physiological maturity with the incorporation of the weather forecast (nRMSE ~8.33%) was comparable with actual weather input (nRMSE ~7.83%) (Fig. 6). The progressive LAI assimilation (from 1 to 3) along with either actual or forecasted weather did not significantly influence the overall nRMSE in days to anthesis and physiological maturity. The simulated days to anthesis was overestimated by the proposed framework when only the first LAI is assimilated along with either actual or forecasted weather (Supplementary Fig. S11). The degree of overestimation in simulated days to anthesis decreased with the assimilation of LAI on subsequent dates. The simulated days to physiological maturity was both under and over-estimated by the proposed framework when only the first LAI is assimilated along with either actual weather or forecasted weather (Supplementary Fig. S12). The simulated days to physiological maturity was underestimated with the assimilations of LAI in subsequent days.

The error in simulating total dry matter was slightly higher with the incorporation of weather forecast than with actual weather input (Fig. 6). It was observed that progressive LAI assimilations (from 1 to 2) along with the incorporation of either actual or forecasted weather

significantly reduced the nRMSE by 2% and 6% in total dry matter in the 2015–16 and 2016–17 seasons, respectively. However, the third progressive assimilation of LAI did not further significantly reduce nRMSE in total dry matter. The simulated total dry matter was under-estimated mainly by the proposed framework when only the first LAI is assimilated along with either actual weather or forecasted weather (Supplementary Fig. S13). The degree of underestimation decreased with the subsequent assimilations of LAI.

It was observed that progressive LAI assimilations (from 1 to 2) along with the incorporation of either actual or forecasted weather significantly reduced the nRMSE by 5–7% in grain yield (Fig. 6). Progressive third assimilation of LAI further significantly reduced nRMSE by 5% in grain yield. The proposed framework's simulated grain yield was underestimated when only the first LAI was assimilated along with either actual or forecasted weather in the season 2016–17 while it was overestimated in the season 2015–16 (Supplementary Fig. S14). Overall, both the underestimation and overestimation in grain yield decreased significantly with the progressive assimilation of LAI.

11.6. Model simulation with all measured inputs versus modified Infocrop-LAI assimilation-weather forecast framework with standard management inputs

Table 6 shows that the proposed framework (modified Infocrop-LAI assimilation-Weather Forecast framework) could simulate days to anthesis with only 2% higher nRMSE with standard inputs than with all actual measured inputs. Similarly, the error was higher by 5% in physiological maturity, 3% higher in dry matter and 1% higher in grain yield. Overall, the proposed framework with standard management inputs could simulate phenology, dry matter and yield of wheat without an appreciable increase in error compared to all measured inputs, thus indicating the workability of the framework to compensate for errors due to the non-availability of actual field measured inputs.

11.7. Spatial distribution of forecasted model outputs

The proposed forecasting framework was run pixel by pixel for the study region, and spatial maps were generated for days to anthesis, days to physiological maturity, total dry matter and grain yield for both 2015–16 and 2016–17 seasons. The spatial maps of grain yield are illustrated in Fig. 7. The maps of other parameters are provided in Supplementary material section 2.4. The maps show a large spatial and inter-annual variability in days to anthesis and physiological maturity, total dry matter and grain yield in the study region. The maps also show that the maximum differences between AW and FW simulations were under LAI1 scenario and these differences narrowed with the progressive LAI assimilation in LAI2 and LAI3 scenarios.

Table 5
Verification measures for WRF model forecasting accuracy and bias-corrected forecasts.

		Tmax (°C)		Tmin (°C)		SR (kJ/m ² /day)		AVP (kPa)		WS (m/s)		
		I	II	I	II	I	II	I	II	I	II	
<i>r</i>	RMSE	WBC	5.78	3.61	3.71	2.90	6693.61	4776.78	0.51	0.51	1.82	1.83
		NWABC	2.47	2.20	2.98	2.55	2805.34	2698.75	0.21	0.21	0.92	0.90
		WBAC	1.94	1.90	2.36	2.14	2391.77	2324.50	0.17	0.18	0.80	0.79
MSB	WBC	0.82	0.85	0.82	0.74	0.81	0.74	0.70	0.59	0.38	0.46	
	NWABC	0.85	0.86	0.74	0.80	0.86	0.84	0.68	0.73	0.30	0.44	
	WBAC	0.91	0.90	0.83	0.86	0.96	0.88	0.78	0.82	0.41	0.47	
MAE	WBC	-4.40	-2.80	-1.38	-0.34	-5916.02	-3542.71	0.47	0.44	-1.53	-1.55	
	NWABC	-0.30	-0.13	-0.09	0.21	-18.95	337.08	0.02	0.02	-0.04	-0.06	
	WBAC	-0.17	-0.09	-0.05	0.14	-18.48	200.93	0.01	0.01	-0.03	-0.04	
	WBC	4.48	2.90	2.76	2.39	5900.75	3935.71	0.46	0.44	1.58	1.56	
	NWABC	1.80	1.60	2.22	1.94	2279.32	1986.39	0.16	0.12	0.68	0.73	
	WBAC	1.40	1.36	1.76	1.61	1943.96	1715.09	0.14	0.10	0.59	0.65	

WBC – without bias correction; NWABC – non-weighted adaptive bias correction; WABC - weighted adaptive bias correction; I – season 2015–16; II – season 2016–17. Tmax- daily maximum air temperature; Tmin – daily minimum air temperature; SR – solar radiation; AVP – actual vapor pressure; WS – wind speed.

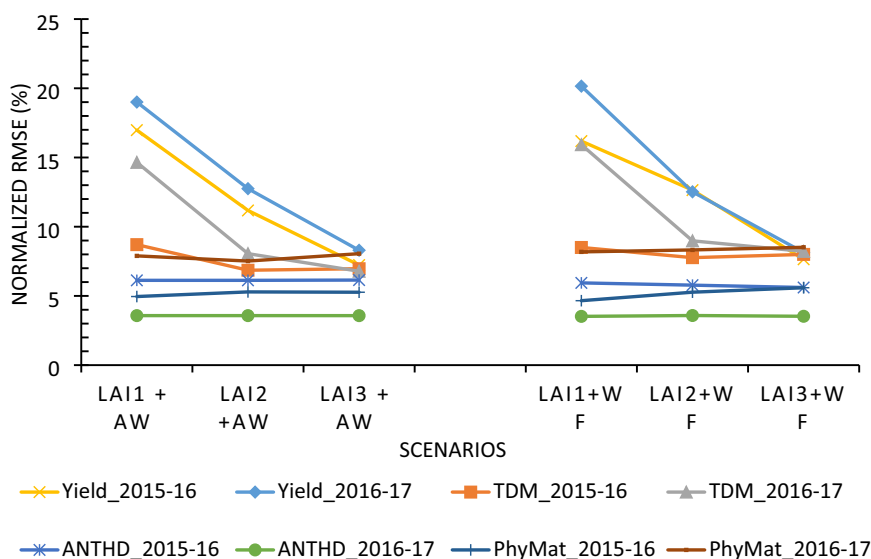


Fig. 6. Evaluation of modified model-LAI assimilation-weather forecast framework in terms of nRMSE for days to anthesis, days to physiological maturity, total dry matter and grain yield. LAI1: LAI assimilation on first date; LAI2: LAI assimilation on first and second date; LAI3: LAI assimilation on first, second and third date; AW: actual weather; WF: forecasted weather (Experiment details are provided in Table 3).

Table 6

Comparing the errors in model simulated outputs with all the measured inputs versus modified Infocrop-LAI assimilation-Weather Forecast framework with the standard management inputs.

Parameters [#]	RMSE		nRMSE (%)	
	All measured inputs + AW	Standard inputs + LAI & WF assimilation	All measured inputs + AW	Standard inputs + LAI & WF assimilation
ANTD (days)	3.0	4.66	3	5
PhyM (days)	3.0	9.0	2	7
TDM (kg/ha)	598	1072	5	8
GY (kg/ha)	361	409	7	8

AW: Actual weather; WF: Forecasted weather.

[#] ANTD- days to anthesis; PhyM- physiological maturity; TDM- total dry matter; GY – grain yield.

Markedly different pattern in simulated grain yield was observed in both cases of assimilation in the framework (1) LAI + actual weather and (2) LAI + weather forecast (Fig. 7). The dominated grain yield category in LAI3 assimilations was 3.5–5.0 t/ha in 2015–16, while it was dominated by 5.5 to 6.5 t/ha in 2016–17.

12. Discussion

Developing a field-scale spatial crop yield forecasting system under limited field data availability for a large area is needed for a range of applications, like, crop insurance, agro-advisory, supply chain management, food security, resource allocation, etc. This study aimed at developing such a forecasting system for the wheat crop integrating scientific advances made in the fields of simulation modelling, remote sensing and weather forecasting. The proposed system has crop simulation model at its center with in-season field information on remote sensing derived crop LAI getting assimilated into the simulation model to steer the model and also integrates information on crop management, weather – actual or forecasted, etc. It is also apparent that output from each component of the system is not free from their independent error. It is highly uncertain how these errors will propagate into the system output. Therefore, evaluating the output from such a system is very

important, and prior to that, an appropriate selection of each component is also imperative.

The first key element of the system is the selection of CSM. In this study, we chose the InfoCrop model for simulating the growth, development and yield of wheat crop due to following reasons: (i) it can overcome the limitation of empirical models due to its dynamic mechanistic nature, (ii) it is indigenously developed model which is suitably calibrated and validated for Indian wheat (Aggarwal et al., 2006), (iii) availability of source code of the model, and (iv) InfoCrop like other CSMs simulate the leaf growth in terms of LAI which can be taken as coupling point of remote sensing information and crop model. Because LAI is one of the widely used variables for assimilation in crop models due to its vital role in radiation interception, CO₂ assimilation, dry matter accumulation and yield, thus, it is a comprehensive indicator of the effect of weather, management and genotype on crop growth and yield (Curnel et al., 2011; Huang et al., 2016; Vazifedoust et al., 2009; Wang et al., 2013).

The second key aspect of the system is the retrieval of LAI from remote sensing. This study chose PROSAIL canopy RTM as it is considered to be well suited for relatively homogenous crop canopies such as wheat (Dhakar et al., 2019b; Jacquemoud et al., 2009; Sehgal et al., 2016). LUT based inversion of the PROSAIL model was used to retrieve LAI as it can overcome the site-specificity and insensitivity of vegetation indices at higher LAI, thus leading to higher accuracy over empirical methods (Dhakar et al., 2019b; Houborg and Boegh, 2008; Kimes et al., 2000; Sehgal et al., 2016).

The third crucial aspect of the system is the strategy of LAI assimilation in the CSM. The Forcing and EnKF strategies were selected because they are easier to implement and computationally efficient than reinitialization/re-calibration strategies of LAI assimilation, but penalize the internal coherence of the system as it causes discontinuities in state variables (Bouman, 1995; Jin et al., 2018; Zhao et al., 2013). Therefore, the model was modified in such a way that it not only maintained the internal coherence of the system but also took less computational time. Among the sequential data assimilation algorithms, EnKF was selected because of its considerable success in implementation into agro-hydrological models (Curnel et al., 2011; Ines et al., 2013) as it accounted for uncertainties in both observations and the model itself. The fourth key element of the system is the incorporation of weather forecasts into CSM. We used Weather Research and Forecasting (WRF) model (Skamarock et al., 2016) for generating weather forecast due to

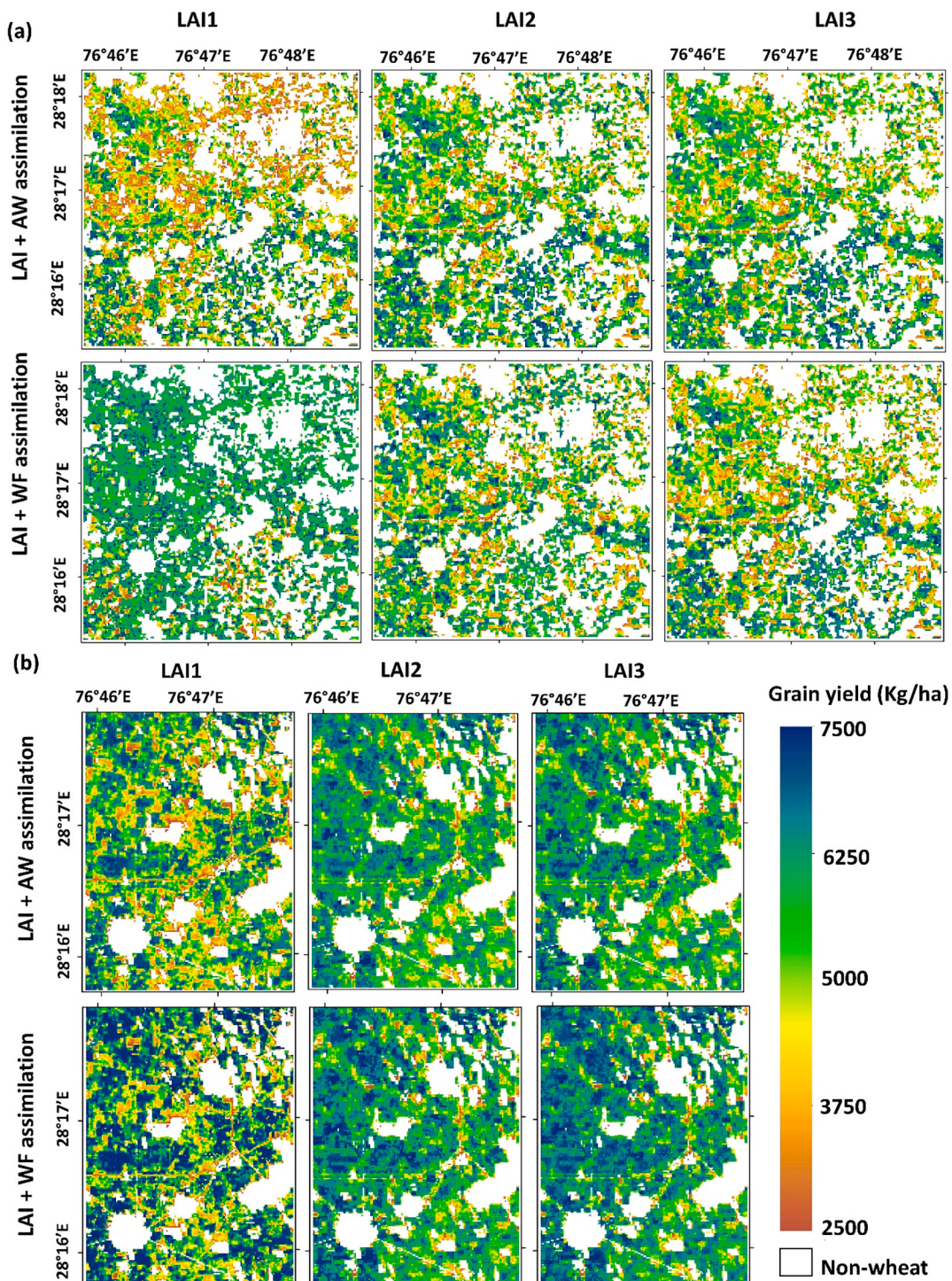


Fig. 7. Maps of simulated grain yield for (a) 2015–16 and (b) 2016–17, by the proposed framework with actual weather (AW) and forecasted weather (WF) along with progressive LAI assimilation (LAI1, 2, 3).

the following reasons: (i) dynamical nature of the model and open-source, (ii) it is one of the unique models providing solar radiation which can be directly used in CSM, and (iii) can be run for the desired length of forecast periods and spatio-temporal resolution. Weather forecast from the WRF model is also not free from error and contain systematic biases (Auligné et al., 2007; Roberts, 2008). These biases have to be corrected before their use in CSM.

LAI retrieval through LUT based PROSAIL inversion from Landsat-8 OLI and Sentinel-2A MSI was achieved with acceptable accuracy (RMSE

$\sim 0.5 \text{ m}^2/\text{m}^2$). The results are in conformity with those reported by Sehgal et al. (2016). Model validation showed that the InfoCrop could simulate growth, development and yield of wheat at farmers' fields with reasonable accuracy (Dhakar et al., 2019a), and so can be utilized further in the regional yield forecasting framework.

At first, we modified the InfoCrop model without correcting for developmental stages/phenology. The modified model with LAI assimilation simulated total dry matter and yield with reasonable accuracy with uniform standard management inputs only when the actual date of

sowing was supplied to the model. After that also, we encountered several issues in accurately simulating the yield with the LAI assimilation alone and standard management inputs. It was observed that LAI assimilation without phenology correction led to unusual higher total dry matter and yield, especially with the Forcing assimilations in the late sown crop. The underlying reason was that 3rd LAI assimilation in late sown crop coincided with anthesis to grain filling stage (schematically illustrated in Fig. 8). The higher LAI during anthesis to grain filling stage led to ample photo-assimilates that mobilized without limitation towards the sink and also in structural reserve, ultimately resulting in unusually higher total dry matter and yield. Curnel et al. (2011) also remarked that the phenological shift between model and observation could substantially influence the model outputs.

To address this issue, we corrected/adjusted the developmental stage (phenology) based on LAI assimilation at the first time step with our novel concept in this study. We demonstrated that phenology adjustment based on LAI assimilation mostly captured the variability in both developmental stages, i.e. anthesis and physiological maturity at farmers' fields. Estimating phenology based on LAI assimilation using crop simulation model will also add immense value in crop phenology based applications like agromet advisory services, resource management, crop yield predictions, yield gap assessment, climate change studies, etc.

We assumed that other state variables like leaf weight, stem weight, root weight, storage organ weight, storage organ number, crop nitrogen demand and uptake etc., change in proportion to assimilated LAI change to maintain the functional coherence of the model (Sehgal et al., 2002). Sehgal et al. (2002) also attempted to modify the WTGROWS wheat model's state variables in proportion to LAI change using the Forcing method. They showed considerable success in simulating wheat yield at the regional level. We could have reinitialized the model to update the other state variables, but our aim of model modification was also to keep it computationally efficient in terms of time and memory use. All other model state variables may not vary in the same proportion as the change in LAI, which could be one of the limitations of the model modification strategy. As the final output of phenology, total dry matter and yield were predicted with acceptable errors by this strategy, so it was taken to be working. Correcting all other state variables using different approaches (other than proportional change) may have scope to improve

the model outputs further.

Modified model – LAI assimilation framework was tested with the assimilation of different scenarios of crop growth (Supplementary material Table S1). It was noticed that the framework simulated almost the same phenology under both Forcing and EnKF LAI assimilation, except for the high crop growth throughout the season (scenario 9). It was observed that high LAI assimilation through Forcing did not result in a corresponding increase in days to anthesis and physiological maturity i.e., equivalent to open-loop simulation. Because high LAI during booting to grain filling stage caused moderate water stress and partial N stress, which impeded the increase in days to anthesis and physiological maturity. The results of all LAI scenarios showed that higher grain yield was obtained in Forcing simulation than in EnKF simulation except for scenario 9 (high LAI) and scenario 7 (low LAI in later period growth). It may be due to the fact that assimilated LAI through Forcing was always higher than EnKF (when model simulated LAI was less than observed LAI), which led to more production of photosynthates and its mobilization towards grains. Forcing under scenario 7 caused low LAI than EnKF during the grain filling stage, which caused lower grain yield. In scenario 9, high LAI during the grain filling stage due to Forcing caused partial water and N stress resulting in lowered yield than EnKF.

Previous studies have shown that assimilation of LAI through ensemble Kalman filter improved the crop yield performance compared to that without LAI assimilation (Curnel et al., 2011; Ines et al., 2013). In addition, our study demonstrated that assimilation of LAI through EnKF improved not only crop yield prediction but also phenology and growth of wheat with our novel approach even when using standard management inputs.

Few studies have incorporated the weather forecast from a dynamical weather model into crop models for phenology and crop yield forecasting (Archontoulis et al., 2016; Togliatti et al., 2017). We are yet to come across any study that integrated the dynamical weather forecast and LAI assimilation into crop model. We also evaluated how the two bias correction methods minimized the systematic biases in the deterministic weather forecast. The result showed that logarithmic weighted adaptive bias correction outperforms non-weighted bias correction for 15 days lead time. The reason for better performance of weighted bias correction is due to the fact that proximate past weather resembles more to present weather than the distant past according to logarithmic

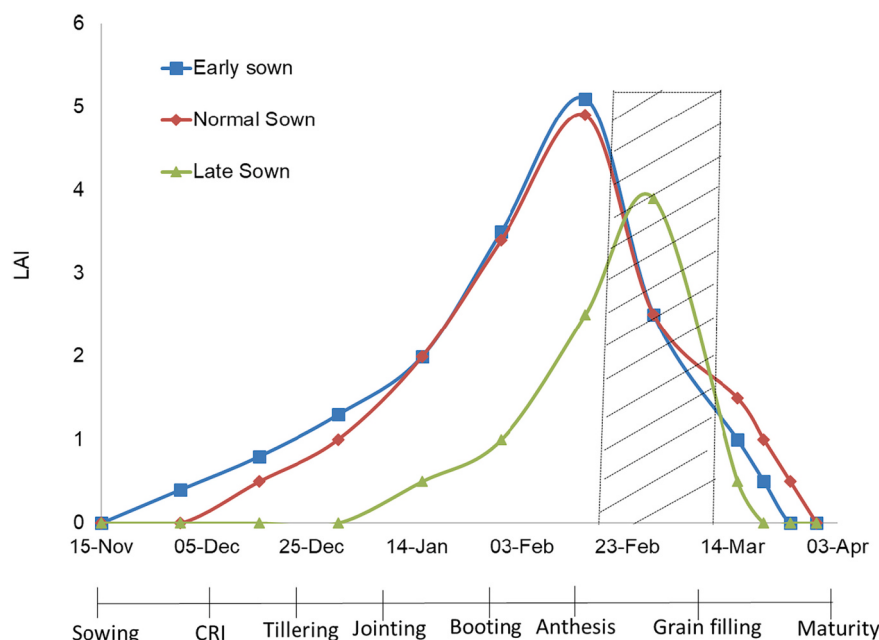


Fig. 8. Schematic diagram showing that late sown crop coincides with anthesis to grain filling stages when LAI is assimilated into CSM with standard management inputs but without phenology adjustment.

weightage. Bias correction was not performed on forecasted precipitation as wheat is mostly grown under full irrigation and is little affected by the precipitation.

Weighted adaptive bias corrected weather forecast and LAI assimilation through EnKF was incorporated into the modified InfoCrop model-LAI assimilation framework. The errors in simulating physiological maturity were higher when incorporated the weather forecast (even though bias-corrected) due to lower accuracy of temperature forecast. Higher maximum temperature led to the forced maturity of the crop. Our results also showed that progressive LAI assimilation (1 to 3 times) improved the phenology, dry matter and yield predictions. However, assimilation of 3rd LAI (coincided with the anthesis to grain filling stages) did not further improve significantly the total dry matter prediction but for grain yield. It implies that LAI assimilation during anthesis to grain filling stage is very important for improved grain yield prediction. Zhang et al. (2016) also showed that the heading or anthesis stage of wheat is the best coupling stage for good yield prediction by integrating WheatGrow and PROSAIL models.

In summary, we demonstrated a novel wheat growth and yield forecasting system assimilating LAI through ensemble Kalman filter and bias-corrected weather forecast from dynamical WRF model into InfoCrop-wheat model, which can also be run spatially. The workable prototype system has shown acceptable accuracy in forecasting phenology, total dry matter and yield of spring wheat at field scale even under limited field data availability. A point-scale implementation of the prototype system is available on the website <http://creams.iari.res.in> as a downloadable CAFS Application.

13. Conclusions

Monitoring and forecasting phenology, growth and yield of a crop is an essential component of food security across the globe. This study shows the novel fusion of crop simulation model, remote sensing and weather forecasting technologies to monitor and forecast phenology, growth and yield of the wheat crop at farmers' field scale under limited field data availability. We modified the InfoCrop-wheat model to allow for LAI assimilation in the model itself, which led the model to follow a correct simulation pathway with high computational efficiency and developed the modified InfoCrop-LAI assimilation framework through successful implementation of Ensemble Kalman filter and Forcing algorithms of multiple LAI assimilations. The in-season assimilation of remote sensing derived LAI into the model compensates for model errors on account of providing standard inputs for each field. We demonstrated the correction of the developmental stage (phenology) based on LAI assimilation with our novel concept and is essential for the improved performance of the system. Our study demonstrated that assimilation of LAI through EnKF improved not only crop yield prediction performance but also phenology and growth of wheat even with standard management inputs. Thus, our strategy of LAI assimilations eliminates the large management input data requirement, which is difficult to obtain for farmers' fields over a region. The study also demonstrated that among the bias correction methods of WRF weather forecasts, weighted adaptive bias correction outperforms non-weighted bias correction for 15 days lead time and hence may be adopted in different quantitative applications. With the systematic experience of this study, the prototype may be adopted by different stakeholders for real-time crop conditions and damage assessment of wheat at farmers' field scale. This information offers considerable potential for improved crop assessment within the marginal and smallholder systems, which are important for crop insurance schemes, supporting resilient farming against aberrant weather situations.

Disclosure statement

No conflict of interest.

Funding

This work was funded by ICAR-National Innovations on Climate Resilient Agriculture (NICRA) project and IARI in-house project [CRSCIARISIL2014028260].

Declaration of Competing Interest

None.

Acknowledgements

The first author acknowledges his employer for granting study leave to undertake PhD. Authors acknowledge the research facilities extended by Head, Division of Agricultural Physics, Indian Agricultural Research Institute, New Delhi. The guidance provided by Dr. V.K. Dadhwal, Director, IIST (ISRO), Trivendrum and Dr. P.K. Aggarwal, CCAFS – South Asia, New Delhi is duly acknowledged. We thank the anonymous reviewers and editors for their many insightful comments and suggestions to improve the manuscript.

Appendix A. Supplementary data

Supplementary data to this article can be found online at <https://doi.org/10.1016/j.agrsy.2021.103299>.

References

- Aggarwal, P.K., Kalra, N., Chander, S., Pathak, H., 2006. InfoCrop: a dynamic simulation model for the assessment of crop yields, losses due to pests, and environmental impact of agro-ecosystems in tropical environments. I. Model description. Agric. Syst. 89, 1–25. <https://doi.org/10.1016/j.agrsy.2005.08.001>.
- Archontoulis, S., Licht, M., Castellano, M., Dietzel, R., Van Looocke, A., Ordóñez, R., Iqbal, J., Puntel, L., Cordova, C., Togliatti, K., Martinez-Feria, R.A., Isaiah, H., Helmers, M., 2016. Understanding the 2016 yields and interactions between soils, crops, climate and management. In: Proceedings of the Integrated Crop Management Conference. Iowa State University, digital press. <https://doi.org/10.31274/icm-180809-279>.
- Auligné, T., McNally, A.P., Dee, D.P., 2007. Adaptive bias correction for satellite data in a numerical weather prediction system. Q. J. R. Meteorol. Soc. 133, 631–642. <https://doi.org/10.1002/qj.56>.
- Bach, H., Mauser, W., 2003. Methods and examples for remote sensing data assimilation in land surface process modeling. IEEE Trans. Geosci. Remote Sens. 41, 1629–1637. <https://doi.org/10.1109/TGRS.2003.813270>.
- Bolten, J.D., Crow, W.T., Zhan, X., Jackson, T.J., Reynolds, C.A., 2010. Evaluating the utility of remotely sensed soil moisture retrievals for operational agricultural drought monitoring. IEEE J. Sel. Top. Appl. Earth Obs. Remote Sens. 3, 57–66. <https://doi.org/10.1109/JSTARS.2009.2037163>.
- Bouman, B.A., 1995. Crop Modelling and remote sensing for yield prediction. Neth. J. Agric. Sci. 43, 143–161. <https://doi.org/10.18174/njas.v43i2.573>.
- Carberry, P.S., Hochman, Z., Hunt, J.R., Dalgleish, N.P., McCown, R.L., Whish, J.P.M., Robertson, M.J., Foale, M.A., Poulton, P.L., van Rees, H., 2009. Re-inventing model-based decision support with Australian dryland farmers. 3 Relevance of APSIM to commercial crops. Crop Pasture Sci 60, 1044. <https://doi.org/10.1071/CP09052>.
- Chipanshi, A., Zhang, Y., Kouadio, L., Newlands, N., Davidson, A., Hill, H., Warren, R., Qian, B., Daneshfar, B., Bedard, F., Reichert, G., 2015. Evaluation of the integrated Canadian crop yield forecaster (ICCYF) model for in-season prediction of crop yield across the Canadian agricultural landscape. Agric. For. Meteorol. 206, 137–150. <https://doi.org/10.1016/j.agrformet.2015.03.007>.
- Crow, W.T., Wood, E.F., 2003. The assimilation of remotely sensed soil brightness temperature imagery into a land surface model using ensemble Kalman filtering: a case study based on ESTAR measurements during SGP97. Adv. Water Resour. 26, 137–149. [https://doi.org/10.1016/S0309-1708\(02\)00088-X](https://doi.org/10.1016/S0309-1708(02)00088-X).
- Curnel, Y., de Wit, A.J.W., Duveiller, G., Defourny, P., 2011. Potential performances of remotely sensed LAI assimilation in WOFOST model based on an OSS experiment. Agric. For. Meteorol. 151, 1843–1855. <https://doi.org/10.1016/j.agrformet.2011.08.002>.
- Das, N.N., Mohanty, B.P., Cosh, M.H., Jackson, T.J., 2008. Modeling and assimilation of root zone soil moisture using remote sensing observations in walnut gulch watershed during SMEX04. Remote Sens. Environ. 112, 415–429. <https://doi.org/10.1016/j.rse.2006.10.027>.
- de Wit, A.J.W., van Diepen, C.A., 2007. Crop model data assimilation with the ensemble Kalman filter for improving regional crop yield forecasts. Agric. For. Meteorol. 146, 38–56. <https://doi.org/10.1016/j.agrformet.2007.05.004>.
- Delécolle, R., Maas, S.J., Guérif, M., Baret, F., 1992. Remote sensing and crop production models: present trends. ISPRS J. Photogramm. Remote Sens. 47, 145–161. [https://doi.org/10.1016/0924-2716\(92\)90030-D](https://doi.org/10.1016/0924-2716(92)90030-D).

- Dente, L., Satalino, G., Mattia, F., Rinaldi, M., 2008. Assimilation of leaf area index derived from ASAR and MERIS data into CERES-wheat model to map wheat yield. *Remote Sens. Environ.* 112, 1395–1407. <https://doi.org/10.1016/j.rse.2007.05.023>.
- Dhakar, R., Sehgal, V.K., Chakraborty, D., Mukherjee, J., Kumar, S.N., 2019a. Evaluating infocrop model for growth, development and yield of spring wheat at farmers' field in semi-arid environment. *J Agrometeorol* 21, 254–261.
- Dhakar, R., Sehgal, V.K., Chakraborty, D., Sahoo, R.N., Mukherjee, J., 2019b. Field scale wheat LAI retrieval from multispectral sentinel 2A-MSI and LandSat 8-OLI imagery: effect of atmospheric correction, image resolutions and inversion techniques. *Geocarto Int.* 1–21. <https://doi.org/10.1080/10106049.2019.1687591>.
- Dhakar, R., Sehgal, V.K., Chakraborty, D., Mukherjee, J., S.N.K., 2021. Calibration and validation of InfoCrop model for phenology, LAI, dry matter and yield of wheat. *Indian J. Agric. Sci.* 91, 115–119.
- Doraiswamy, P.C., Moulin, S., Cook, P.W., Stern, A., 2003. Crop yield assessment from remote sensing. *Photogramm. Eng. Remote. Sens.* 69, 665–674. <https://doi.org/10.14358/PERS.69.6.665>.
- Dorigo, W.A., Zurita-Milla, R., de Wit, A.J.W., Brazile, J., Singh, R., Schaepman, M.E., 2007. A review on reflective remote sensing and data assimilation techniques for enhanced agroecosystem modeling. *Int. J. Appl. Earth Obs. Geoinf.* 9, 165–193. <https://doi.org/10.1016/j.jag.2006.05.003>.
- Dunne, S., Entekhabi, D., 2005. An ensemble-based reanalysis approach to land data assimilation. *Water Resour. Res.* 41. <https://doi.org/10.1029/2004WR003449>.
- ENVI, 2009. ENVI Atmospheric Correction Module: QUAC and FLAASH user's Guide. Modul. Version.
- Evensen, G., 2003. The Ensemble Kalman Filter: Theoretical formulation and practical implementation. *Ocean Dyn.* <https://doi.org/10.1007/s10236-003-0036-9>.
- Fang, H., Liang, S., Hoogenboom, G., 2011. Integration of MODIS LAI and vegetation index products with the CSM-CERES-maize model for corn yield estimation. *Int. J. Remote Sens.* 32, 1039–1065. <https://doi.org/10.1080/01431160903505310>.
- Fischer, A., Kergoat, L., Dedieu, G., 1997. Coupling satellite data with vegetation functional models: review of different approaches and perspectives suggested by the assimilation strategy. *Remote Sens. Rev.* 15, 283–303. <https://doi.org/10.1080/0275725970953243>.
- Hadria, R., Duchemin, B., Lahrouni, A., Khabba, S., Er-raki, S., Dedieu, G., Chehbouni, A. G., Olioso, A., 2006. Monitoring of irrigated wheat in a semi-arid climate using crop modelling and remote sensing data: impact of satellite revisit time frequency. *Int. J. Remote Sens.* 27, 1093–1117. <https://doi.org/10.1080/01431160500382980>.
- Hansen, J., Challinor, A., Ines, A., Wheeler, T., Moron, V., 2006. Translating climate forecasts into agricultural terms: advances and challenges. *Clim. Res.* 33, 27–41. <https://doi.org/10.3354/crc03027>.
- Huang, J., Sedano, F., Huang, Y., Ma, H., Li, X., Liang, S., Tian, L., Zhang, X., Fan, J., Wu, W., 2016. Assimilating a synthetic Kalman filter leaf area index series into the WOFOST model to improve regional winter wheat yield estimation. *Agric. For. Meteorol.* 216, 188–202. <https://doi.org/10.1016/j.agrformet.2015.10.013>.
- Houborg, R., Boegh, E., 2008. Mapping leaf chlorophyll and leaf area index using inverse and forward canopy reflectance modeling and SPOT reflectance data. *Remote Sens. Environ.* 112, 186–202. <https://doi.org/10.1016/j.rse.2007.04.012>.
- Huang, J., Ma, H., Sedano, F., Lewis, P., Liang, S., Wu, Q., Su, W., Zhang, X., Zhu, D., 2019. Evaluation of regional estimates of winter wheat yield by assimilating three remotely sensed reflectance datasets into the coupled WOFOST-PROSAIL model. *Eur. J. Agron.* 102, 1–13. <https://doi.org/10.1016/j.eja.2018.10.008>.
- Ines, A.V.M., Das, N.N., Hansen, J.W., Njoku, E.G., 2013. Assimilation of remotely sensed soil moisture and vegetation with a crop simulation model for maize yield prediction. *Remote Sens. Environ.* 138, 149–164. <https://doi.org/10.1016/j.rse.2013.07.018>.
- Jacquemoud, S., Verhoef, W., Baret, F., Bacour, C., Zarco-Tejada, P.J., Asner, G.P., François, C., Ustin, S.L., 2009. PROSPECT+SAIL models: a review of use for vegetation characterization. *Remote Sens. Environ.* 113, S56–S66. <https://doi.org/10.1016/j.rse.2008.01.026>.
- Jin, X., Kumar, L., Li, Z., Feng, H., Xu, X., Yang, G., Wang, J., 2018. A review of data assimilation of remote sensing and crop models. *Eur. J. Agron.* 92, 141–152. <https://doi.org/10.1016/j.eja.2017.11.002>.
- Kalman, R.E., 1960. A new approach to linear filtering and prediction problems. *J. Basic Eng.* 82, 35–45. <https://doi.org/10.1115/1.3662552>.
- Kamble, B., Irmak, A., Hubbard, K., Gowda, P., 2013. Irrigation scheduling using remote sensing data assimilation approach. *Adv. Remote Sens.* 02, 258–268. <https://doi.org/10.4236/ars.2013.23028>.
- Keppenne, C.L., Rienerker, M.M., 2002. Initial testing of a massively parallel ensemble Kalman filter with the Poseidon Isopycnal Ocean general circulation model. *Mon. Weather Rev.* 130, 2951–2965. [https://doi.org/10.1175/1520-0493\(2002\)130<2951:ITOAMP>2.0.CO;2](https://doi.org/10.1175/1520-0493(2002)130<2951:ITOAMP>2.0.CO;2).
- Kimes, D.S., Knyazikhin, Y., Privette, J.L., Abuelgasim, A.A., Gao, F., 2000. Inversion methods for physically-based models. *Remote Sens. Rev.* 18, 381–439. <https://doi.org/10.1080/02757250009532396>.
- Kumar, A., Singh, R., Singh, G., Sharma, R.K., Saharan, M.S., Chhokar, R.S., Tyagi, B.S., Sendhil, R., Chand, R., Sharma, I., 2014. Wheat cultivation in India (pocket guide). Direct. Wheat Res. Karnal 132, 001. <https://iiwbr.icar.gov.in/wp-content/uploads/2018/02/EB-52-Wheat-Cultivation-in-India-Pocket-Guide.pdf>.
- Li, X., Bai, Y., 2013. Assimilating remote sensing data into land surface models: theory and methods, in land surface observation, modeling and data assimilation. *World Scientific* 143–170. https://doi.org/10.1142/9789814472616_0006.
- Lunagaria, M.M., Patel, H.R., 2019. Evaluation of PROSAIL inversion for retrieval of chlorophyll, leaf dry matter, leaf angle, and leaf area index of wheat using spectrodirectional measurements. *Int. J. Remote Sens.* 40, 8125–8145. <https://doi.org/10.1080/01431161.2018.1524608>.
- Ma, G., Huang, J., Wu, W., Fan, J., Zou, J., Wu, S., 2013. Assimilation of MODIS-LAI into the WOFOST model for forecasting regional winter wheat yield. *Math. Comput. Model.* 58, 634–643. <https://doi.org/10.1016/j.mcm.2011.10.038>.
- Maas, S.J., 1988. Use of remotely-sensed information in agricultural crop growth models. *Ecol. Model.* 41, 247–268. [https://doi.org/10.1016/0304-3800\(88\)90031-2](https://doi.org/10.1016/0304-3800(88)90031-2).
- Makowski, D., Guerif, M., Jones, J.W., Graham, W., Wallach, D., 2006. Data assimilation with crop models. In: Wallach, D., Makowski, D., Jones, J.W. (Eds.), *Working with Dynamic Crop Models: Evaluation, Analysis, Parameterization, and Applications*. Elsevier, pp. 151–170.
- McLaughlin, D., 2002. An integrated approach to hydrologic data assimilation: interpolation, smoothing, and filtering. *Adv. Water Resour.* 25, 1275–1286. [https://doi.org/10.1016/S0309-1708\(02\)00055-6](https://doi.org/10.1016/S0309-1708(02)00055-6).
- Mokhtari, A., Noory, H., Vazifedoust, M., 2018. Improving crop yield estimation by assimilating LAI and inputting satellite-based surface incoming solar radiation into SWAP model. *Agric. For. Meteorol.* 250–251, 159–170. <https://doi.org/10.1016/j.agrformet.2017.12.250>.
- Morell, F.J., Yang, H.S., Cassman, K.G., Van Wart, J., Elmore, R.W., Licht, M., Coulter, J. A., Ciampitti, I.A., Pittelkow, C.M., Brouder, S.M., Thomison, P., Lauver, J., Graham, C., Massey, R., Grassini, P., 2016. Can crop simulation models be used to predict local to regional maize yields and total production in the U.S. Corn Belt? *Field Crop. Res.* 192, 1–12. <https://doi.org/10.1016/j.fcr.2016.04.004>.
- Moulin, S., 1999. Impacts of model parameter uncertainties on crop reflectance estimates: a regional case study on wheat. *Int. J. Remote Sens.* 20, 213–218. <https://doi.org/10.1080/014311699213730>.
- Moulin, S., Bondeau, A., Delecole, R., 1998. Combining agricultural crop models and satellite observations: from field to regional scales. *Int. J. Remote Sens.* 19, 1021–1036. <https://doi.org/10.1080/014311698215586>.
- Nearing, G.S., Crow, W.T., Thorp, K.R., Moran, M.S., Reichle, R.H., Gupta, H.V., 2012. Assimilating remote sensing observations of leaf area index and soil moisture for wheat yield estimates: an observing system simulation experiment. *Water Resour. Res.* 48 <https://doi.org/10.1029/2011WR011420>.
- Pagani, V., Guarneri, T., Busetto, L., Ranghetti, L., Boscetti, M., Movedi, E., Campos-Taberner, M., Garcia-Haro, F.J., Katsantonis, D., Stavrakoudis, D., Ricciardelli, E., Romano, F., Holecz, F., Collivignarelli, F., Granell, C., Castelyn, S., Confalonieri, R., 2019. A high-resolution, integrated system for rice yield forecasting at district level. *Agric. Syst.* 168, 181–190. <https://doi.org/10.1016/j.agry.2018.05.007>.
- Paniconi, C., Marrocù, M., Putti, M., Verbunt, M., 2003. Newtonian nudging for a Richards equation-based distributed hydrological model. *Adv. Water Resour.* 26, 161–178. [https://doi.org/10.1016/S0309-1708\(02\)00099-4](https://doi.org/10.1016/S0309-1708(02)00099-4).
- Reichle, R.H., McLaughlin, D.B., Entekhabi, D., 2002. Hydrologic data assimilation with the ensemble Kalman filter. *Mon. Weather Rev.* 130, 103–114. [https://doi.org/10.1175/1520-0493\(2002\)130<0103:HDAWTE>2.0.CO;2](https://doi.org/10.1175/1520-0493(2002)130<0103:HDAWTE>2.0.CO;2).
- Roberts, N., 2008. Assessing the spatial and temporal variation in the skill of precipitation forecasts from an NWP model. *Meteorol. Appl.* 15, 163–169. <https://doi.org/10.1002/met.57>.
- Sehgal, V.K., Sastry, C.V.S., 2005. Simulating the effect of nitrogen application on wheat yield by linking remotely sensed measurements with wtgrows simulation model. *J. Indian Soc. Remote Sens.* 33, 297–305. <https://doi.org/10.1007/BF02990049>.
- Sehgal, V.K., Rajak, D.R., Chaudhary, K.N., Dadhwal, V.K., 2002. Improved regional yield prediction by crop growth monitoring system using remote sensing derived crop phenology. In: *The International Archives of the Photogrammetry, Remote Sensing and Spatial Information Sciences*, Vol. 34, pp. 329–334. Part 7.
- Sehgal, V.K., Chakraborty, D., Sahoo, R.N., 2016. Inversion of radiative transfer model for retrieval of wheat biophysical parameters from broadband reflectance measurements. *Inf. Process. Agric.* 3, 107–118. <https://doi.org/10.1016/j.inpa.2016.04.001>.
- Skamarock, W.C., Klemp, J.B., Dudhia, J., Gill, D.O., Barker, D.M., Duda, M.G., Huang, X.-Y., Wang, P., Powers, J.G., 2016. ARW Modelling System UserGuide V.3. Book. <https://doi.org/10.5065/D68S4MVH>.
- Togliatti, K., Archontoulis, S.V., Dietzel, R., Puntel, L., VanLoocke, A., 2017. How does inclusion of weather forecasting impact in-season crop model predictions? *Field Crop. Res.* 214, 261–272. <https://doi.org/10.1016/j.fcr.2017.09.008>.
- van Loon, E.E., Troch, P.A., 2002. Tikhonov regularization as a tool for assimilating soil moisture data in distributed hydrological models. *Hydrol. Process.* 16, 531–556. <https://doi.org/10.1002/hyp.352>.
- Vazifedoust, M., van Dam, J.C., Bastiaanssen, W.G.M., Feddes, R.A., 2009. Assimilation of satellite data into agrohydrological models to improve crop yield forecasts. *Int. J. Remote Sens.* 30, 2523–2545. <https://doi.org/10.1080/01431160802552769>.
- Wang, F., Huang, J., Wang, Y., Liu, Z., Peng, D., Cao, F., 2013. Monitoring nitrogen concentration of oilseed rape from hyperspectral data using radial basis function. *Int. J. Digit. Earth* 6, 550–562. <https://doi.org/10.1080/17538947.2011.628414>.
- Williams, K.E., Falloon, P.D., 2015. Sources of interannual yield variability in JULES—crop and implications for forcing with seasonal weather forecasts. *Geosci. Model Dev.* 8, 3987–3997. <https://doi.org/10.5194/gmd-8-3987-2015>.
- Willmott, C.J., 1981. On the validation of models. *Phys. Geogr.* 2, 184–194. <https://doi.org/10.1080/02723646.1981.10642213>.
- Zhang, L., Guo, C.L., Zhao, L.Y., Zhu, Y., Cao, W.X., Tian, Y.C., Cheng, T., Wang, X., 2016. Estimating wheat yield by integrating the WheatGrow and PROSAIL models. *Field Crop. Res.* 192, 55–66. <https://doi.org/10.1016/j.fcr.2016.04.014>.
- Zhao, Y., Chen, S., Shen, S., 2013. Assimilating remote sensing information with crop model using ensemble Kalman filter for improving LAI monitoring and yield estimation. *Ecol. Model.* 270, 30–42. <https://doi.org/10.1016/j.ecolmodel.2013.08.016>.